BIOCHEMISTRY
including biophysical chemistry & molecular biology

Rapid Report

pubs.acs.org/biochemistry

Amyloid Hydrogen Bonding Polymorphism Evaluated by $^{15}N\{^{17}O\}$REAPDOR Solid-State NMR and Ultra-High Resolution Fourier Transform Ion Cyclotron Resonance Mass Spectrometry

Juan Wei,[†] Oleg N. Antzutkin,[‡,§] Andrei V. Filippov,[§] Dinu Iuga,[‡] Pui Yiu Lam,[‡] Mark P. Barrow,[†] Ray Dupree,[‡] Steven P. Brown,[‡] and Peter B. O'Connor*[,†]

[†]Department of Chemistry and [‡]Department of Physics, University of Warwick, Coventry, CV4 7AL, U.K.
[§]Chemistry of Interfaces, Luleå University of Technology, SE-971 87, Luleå, Sweden

Supporting Information

ABSTRACT: A combined approach, using Fourier transform ion cyclotron resonance mass spectrometry (FTICR-MS) and solid-state NMR (Nuclear Magnetic Resonance), shows a high degree of polymorphism exhibited by Aβ species in forming hydrogen-bonded networks. Two Alzheimer's Aβ peptides, Ac-Aβ_{16-22}-NH_2 and Aβ_{11-25}, selectively labeled with ^{17}O and ^{15}N at specific amino acid residues were investigated. The total amount of peptides labeled with ^{17}O as measured by FTICR-MS enabled the interpretation of dephasing observed in $^{15}N\{^{17}O\}$-REAPDOR solid-state NMR experiments. Specifically, about one-third of the Aβ peptides were found to be involved in the formation of a specific >C═^{17}O···H−^{15}N hydrogen bond with their neighbor peptide molecules, and we hypothesize that the rest of the molecules undergo $\pm n$ off-registry shifts in their hydrogen bonding networks.

Structural stability and folding in biological systems is strongly dependent on a network of hydrogen bonds. Building on fundamental insight into amyloid fibril structure provided by other solid-state NMR methods,[1−8] $^{15}N\{^{17}O\}$REAPDOR solid-state NMR has been recently employed in probing >C═O···H−N hydrogen bonding in amyloid fibrils formed by selectively ^{17}O, ^{15}N labeled Alzheimer's amyloid-β (Aβ) peptides.[9] To use this method, ^{17}O enrichment is essential, because of the low natural abundance (0.04%) of the only magnetic isotope of oxygen. Simulations of $^{15}N\{^{17}O\}$REAPDOR dephasing data include the ^{17}O enrichment level as an important parameter in the evaluation of the heteronuclear $^{15}N-^{17}O$ dipole−dipole coupling constants, from which $^{15}N\cdots^{17}O$ internuclear distances and, therefore, the lengths of hydrogen bonds are calculated.[9,10] However, elucidation of the precise degree of the ^{17}O enrichment in peptides from either conventional mass spectrometry (MS) or ^{17}O NMR spectroscopy is a challenge, because of the naturally abundant ^{13}C (1.07%) isotope and an unknown degree of ^{17}O and ^{18}O enrichment in reagents used in peptide synthesis, all leading to a severe overlap in MS patterns from different isotopologues ($^{13}C^{16}O$, $^{12}C^{17}O$, etc.).

^{17}O enrichment of amino acids is usually achieved by the use of ^{17}O enriched water. Then, amino acids are Fmoc protected and used as the input reagent in the fast Fmoc peptide synthesis. Although the initial ^{17}O and ^{18}O enrichment in water could be determined with a high precision, ^{17}O enrichment levels may change during the whole synthetic pathway. Moreover, for the samples of interest in this research, the important value is the ^{17}O enrichment of one specific oxygen atom within an otherwise normal peptide. Most methods one could consider to accurately determine the $^{17}O/^{18}O$ enrichment values would require chemistry such as acid hydrolysis or enzymatic digestion to cleave the peptide into individual amino acids and afterward measure the ^{17}O enrichment of the individual amino acid. However, such strategies run a strong risk of scrambling the ^{17}O labeling position and thus invalidating the measured ^{17}O enrichment information, and such methods generally will also dilute the signal by inclusion of the oxygen atoms from other unlabeled amino acids.

In a mass spectrum, the well resolved isotopic peaks of one molecule representing each isotopologue are called the isotopic fine structure of this molecule.[11] In principle, the fine structure could be separated if the resolution is sufficiently high (typically requiring a resolving power $m/\Delta m_{50\%}$ of 1−5 M at m/z 1000 depending on the elemental composition), but it remains a challenging task for most modern mass spectrometers. Ultrahigh resolution isotopic fine structure separations have to date been achieved using Fourier transform ion cyclotron resonance mass spectrometry (FTICR-MS) on molecules smaller than 1500 Da[12,13] and are particularly focused on the determination of the elemental composition.[14−20]

The two Aβ samples analyzed in this study are Ac-Aβ_{16-22}-NH_2 (Ac-KLV$_{18}$(^{17}O)FF$_{20}$(^{15}N)AE-NH_2, abbreviated as Aβ_{16-22} hereafter) and Aβ_{11-25} (EVHHQKLV$_{18}$(^{17}O)FFA$_{21}$-(U−^{13}C,^{15}N)EDVG), i.e., the same samples as previously studied by $^{15}N\{^{17}O\}$REAPDOR.[9] Here, using FTICR-MS, the total ratio of ^{17}O enrichment in the two samples is determined. Since ^{15}N is labeled (>98%) on Phe20 for Aβ_{16-22} or on Ala21 for Aβ_{11-25}, and similarly ^{13}C is labeled (>99%) on Ala21 for Aβ_{11-25}, the formulas of the two peptides are written as $C_{45}H_{67}O_{10}N_8{}^{15}N$ (Mw 894.498124 Da) and $C_{78}{}^{13}C_3H_{119}O_{23}N_{20}{}^{15}N$ (Mw 1757.885869 Da), respectively. In order to calculate the ratio of ^{17}O labeling, the two peaks corresponding to ^{13}C-substituted and ^{17}O-substituted peptides in the A+1 cluster (second isotopic

Received: October 7, 2015
Revised: March 4, 2016
Published: March 17, 2016

DOI: 10.1021/acs.biochem.5b01095
Biochemistry 2016, 55, 2065−2068

cluster) must be fully resolved for both peptides, where the mass difference (Δm) between $^{13}C^{16}O$ and $^{12}C^{17}O$ is 0.000862 Da.

On the basis of the FTICR-MS results, the levels of ^{17}O enrichment in these samples are about three times larger than those involved in forming the C═^{17}O···H−^{15}N hydrogen bond as determined by $^{15}N\{^{17}O\}$REAPDOR data for the same samples. We hypothesize that this discrepancy is explained by a high degree of amyloid hydrogen bonding polymorphism with off-registry shifts between peptide molecules forming cross-β structures.

Experimental Procedures. All mass spectrometry experiments were carried out on a Bruker 12 T solariX FTICR mass spectrometer using an Infinity cell[21] (Bruker Daltonik, Germany). See SI for experimental details. Additional control experiments and MS/MS data are also included in the SI, Figures S-1−S-9, and detailed peak assignment tables are available as Tables S-1−S-11.

Solid-state NMR experiments were performed on a Bruker Avance III 850 MHz spectrometer using a triple-resonance 2.5 mm double broadband probe (see SI for additional experimental details). Additional NMR control experiments are also included in the SI, Figures S-10−S-15 and Table S-12. $^{15}N\{^{17}O\}$-REAPDOR NMR experiments were performed for ∼2 mg of $A\beta_{16-22}[Val_{18}(^{17}O), Phe_{20}(^{15}N)]$ aggregates prepared in a PBS buffer at pH 7 following protocols described in detail by Balbach et al.[7] and for ∼4 mg of the polymorphic sample of this peptide prepared in an aqueous solution with pH 6.9 adjusted using NaOH(aq) and CH_3COOH(aq) (see SI for details of the sample preparation protocols section S-2 and NMR instrument settings, section S-3). Transmission electron microscope (TEM) images of the fibrils are in the SI, Figure S-16.

Results and Discussion. Figure 1 shows the high resolution isotopic fine structure of the singly charged $A\beta_{16-22}$

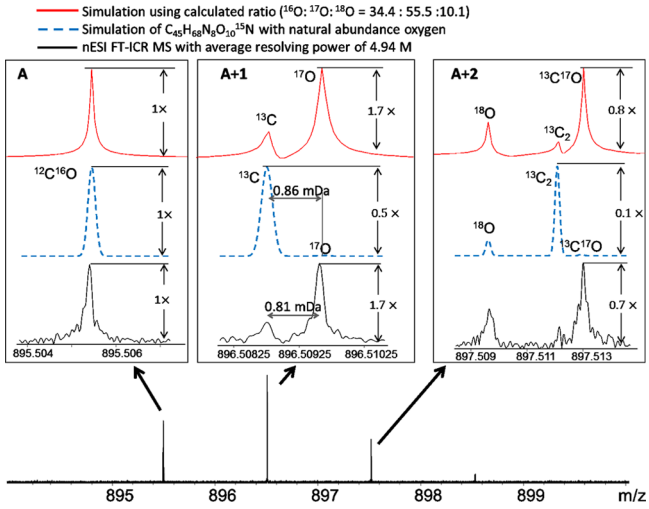

Figure 1. An ultrahigh resolution FTICR mass spectrum of the singly charged $A\beta_{16-22}$ ($C_{45}H_{68}O_{10}N_8{}^{15}N$) in black, and the simulated spectra of $A\beta_{16-22}$ with natural abundance oxygen (dashed blue lines) and using the calculated ratio, ^{16}O: ^{17}O: ^{18}O = 34.4:55.5:10.1 (red lines). The peak list is in Table S-1.

($C_{45}H_{68}O_{10}N_8{}^{15}N$, Mw monoisotopic = 895.505401 Da) including the baseline resolved ^{13}C-substituted ($C_{44}{}^{13}CH_{68}O_{10}N_8{}^{15}N$) and ^{17}O-substituted ($C_{45}H_{68}O_9{}^{17}ON_8{}^{15}N$) peaks in the A+1 cluster. The m/z values of the peaks in Figure 1 are listed in Table S-1 (see Supporting Information) with the monoisotopic peak at m/z 895.505401 as the internal lock mass, and the overall mass uncertainty is 29 ppb. In comparison, the theoretical mass spectrum of the corresponding $A\beta_{16-22}$ peptides with natural abundance oxygen is plotted in Figure 1 as a blue dashed line above the experimental spectrum. With an average experimental resolving power (abbreviated as R.P.) of ∼4.94 M shown in Figure 1, the two peaks in the A+1 cluster are clearly resolved and a 0.000805 Da experimental mass difference is measured which is 57 μDa different from the theoretical value (0.000862 Da).

If the detection of the A+1 cluster with R.P. from 500,000 to 5,000,000 is tracked (shown in Figure S-2), the identification of these two peaks becomes even more apparent. At a R.P. of 500,000, which is still generally not achievable by other types of modern mass spectrometers, the peaks adjacent are completely overlapped. Aided by the fine separation, the ratio of ^{17}O abundance is calculated by

$$^{17}O\ \text{abundance} = I(^{12}C^{17}O)/\{I(^{12}C^{16}O) + I(^{12}C^{17}O) + I(^{12}C^{18}O)\} \quad (1)$$

where $I(^{12}C^{16}O)$, $I(^{12}C^{17}O)$, and $I(^{12}C^{18}O)$ are the ion intensities of the ^{12}C ^{16}O-, ^{12}C ^{17}O-, and ^{12}C ^{18}O- substituted peaks. To minimize the influence of signal fluctuation, the results from six runs are averaged (see Table S-3 in SI), where the experimental ratios of the $^{12}C^{16}O$-, the $^{12}C^{17}O$-, and the $^{12}C^{18}O$-peaks are 34.4 ± 2.3%, 55.5 ± 2.2%, and 10.1 ± 1.3%, respectively (for these $x \pm \Delta x$% values, Δx% is defined as one standard deviation of the uncertainty in the calibration). In contrast, for the corresponding natural abundance oxygen Aβ species, these numbers are 97.6%, 0.4%, and 2% correspondingly. Therefore, in addition to ^{17}O labeling, ^{18}O is also simultaneously detected to be about 8% enrichment for the $A\beta_{16-22}$ peptide. The uncertainty of the measurement is around 2.1% according to the detection of the ^{13}C-species in the same peptide (see SI). The simulated spectrum generated by using the calculated ratio (^{16}O:^{17}O:^{18}O = 34.4:55.5:10.1) is displayed on the top of Figure 1 in red, which matches well with the experimental spectrum on the bottom (black).

With increasing molecular weight, the complexity of elemental composition and the difficulty of isotopic fine structure measurement will increase dramatically. Therefore, the other ^{17}O enriched peptide under study, $A\beta_{11-25}$ ($C_{78}{}^{13}C_3H_{119}O_{23}N_{20}{}^{15}N$), demands an even more challenging isotopic fine structure measurement, since its molecular mass (Mw 1757.885869 Da) is almost twice as much as that of $A\beta_{16-22}$ (Mw 894.498124 Da). Doubly charged $A\beta_{11-25}$ ions are selected, whereby the monoisotopic peak is at m/z 879.950210 ($C_{78}{}^{13}C_3H_{121}O_{23}N_{20}{}^{15}N$). The Δm between the two peaks of interest, the ^{13}C peak ($C_{77}{}^{13}C_4H_{121}O_{23}N_{20}{}^{15}N$), and the ^{17}O peak ($C_{78}{}^{13}C_3H_{121}O_{22}{}^{17}ON_{20}{}^{15}N$) is still the same (0.000862 Da), but $\Delta m/z$ is half, i.e., m/z 0.000431, in this case. Figure 2 shows the ultrahigh resolution fine structure detection for $A\beta_{11-25}$ with an average R.P. of 5.95 M and the corresponding peak list is summarized in Table S-2. The experimental results of the $^{12}C^{16}O$-, $^{12}C^{17}O$-, and $^{12}C^{18}O$-substituted peaks are 27.9%, 56.8%, and 15.3%, respectively (Table S-6).

Additionally, tandem mass spectrometry unambiguously locates the ^{17}O labeling on the carbonyl oxygen of the Val18 residue in $A\beta_{16-22}$ (see Figure S-4 and Table S-8 in SI) and $A\beta_{11-25}$ (Figure S-5 and Table S-8 in SI).

Finally, the oxygen labeling ratio of the Fmoc-Val(^{17}O) (the structure is shown in Figure S-8) sample used in the Fmoc

DOI: 10.1021/acs.biochem.5b01095
Biochemistry 2016, 55, 2065−2068

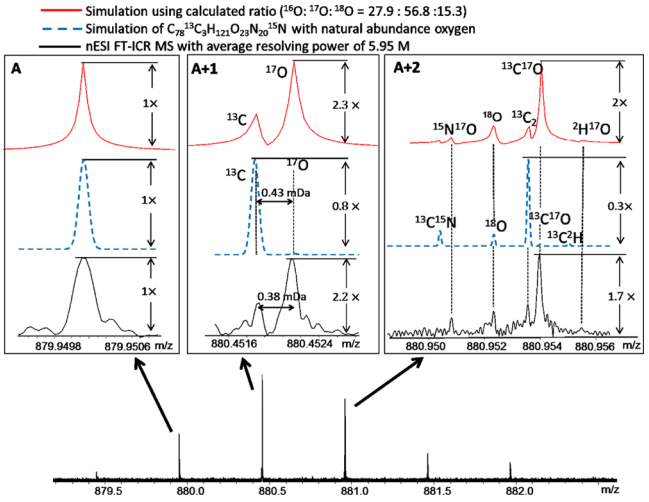

Figure 2. An ultrahigh resolution FTICR mass spectrum of the doubly charged Aβ_{11-25} ($C_{78}{}^{13}C_3H_{121}O_{23}N_{20}{}^{15}N$) in black, and the simulated spectra of Aβ_{11-25} with natural abundance oxygen (dashed blue lines) and using the calculated ratio, ^{16}O: ^{17}O: ^{18}O = 27.9:56.8:15.3 (red lines). The peak list is in Table S-2. Using absorption mode, a further 57% resolution increase was achieved, resulting in RP > 9 M (see Figure S-7 in SI).

synthesis of the two peptides was measured and is estimated to have 27.3 ± 0.9%, 59.4 ± 0.4%, and 13.3 ± 0.8% of ^{16}O, ^{17}O, and ^{18}O respectively (Figure S-9 and Table S-10 in SI). Although the same reagent, Fmoc-Val(^{17}O), was used in the synthesis of both of the peptides, it is not surprising that the ^{17}O labeling values for the peptide products are slightly different from each other and from the labeling value in the amino acid used in the synthesis due to unequal loss during synthesis and storage. Table S-11 summarizes the labeling measurements and experimental uncertainty.

Intriguingly, the amount of ^{17}O in the Ac-Aβ_{16-22}-NH_2 and Aβ_{11-25} is 55−57%, i.e., ca. 3−4 times larger than the 13−15% that we had previously assumed in our analysis of ^{15}N{^{17}O}-REAPDOR MAS NMR data.[9] This discrepancy requires reconsideration of our previous interpretation of dephasing in these ^{15}N{^{17}O}-REAPDOR MAS NMR experiments. Specifically, we, hypothesize here that only a proportion of the peptides in our samples exhibits the registry that brings together in a hydrogen bond C═^{17}O of valine-18 with a ^{15}N labeled NH group of phenylalanine-20 in Aβ_{16-22} or alanine-21 in Aβ_{11-25}, as is required to see a dephasing due to a ^{15}N−^{17}O dipolar coupling. For example, consider Figure 3, which shows, for Aβ_{16-22}, three antiparallel β-sheet arrangements, but with three different registries; i.e., a significant dephasing can only be observed for the 17 + k ←→ 21 − k case in Figure 3b.

To further explore this interpretation, we also present data for an additional sample of amyloid fibrils of [^{15}N,^{17}O]-Aβ_{16-22} using the same batch of the synthesized and purified peptide, but following a modified incubation protocol (see SI). This sample is highly polymorphic in terms of a coexistence of different well-defined secondary structures in the same sample (see TEM images in Figure S-16), since there are at least four different narrow ^{15}N resonance lines readily distinguished between 116 and 130 ppm (see Figures S-12−S-14). ^{15}N{^{17}O}REAPDOR NMR dephasing curves for these different resonances can be fit best using the same dipolar coupling of 80 Hz (corresponding to a C═^{17}O···H−^{15}N hydrogen bond) but different scaling factors

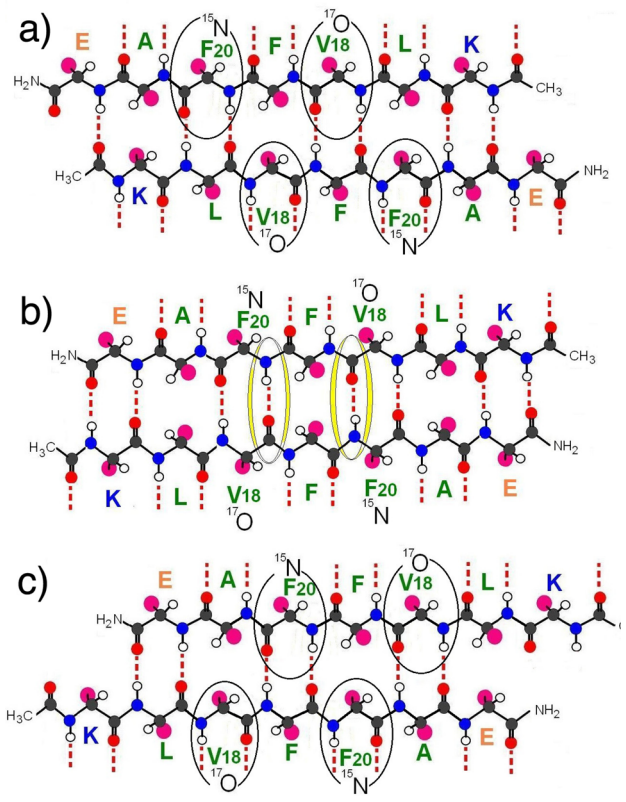

Figure 3. Schematic representation of hydrogen bonding in putative models of amyloid fibrils of Aβ16−22. Three antiparallel arrangements with different registries are exhibited: 17 + k ←→ 20 − k (a); 17 + k ←→ 21 − k (b); 17 + k ←→ 22 − k (c). Experiments are performed on samples with ^{17}O labeling of the Val_{18} carbonyl group and ^{15}N labeling of the Phe_{20} amide group. Selectively isotopically labeled fragments involved in C═^{17}O···H−^{15}N hydrogen bonds are highlighted by yellow ellipsoids in (b) and are absent in (a and c), for which the labeled residues are indicated by black circles.

ranging from 13 to 25% for different resonance lines (see NMR data evaluation in Figure S-15).

In the context of this interpretation of our data, we note that the origin and variety of polymorphism in amyloid fibrils is a widely debated topic.[7,8,22−26] Meier and co-workers have reported on pH-dependent polymorphism of the ccβ-p model peptide, Ac-SIRELEARIRELELRIG-NH_2, which adopts β-pleated structures with different registries: "−2"-or registry at pH 2.0 and "+3"-or registry at pH 7.3.[24] Interestingly, solid-state ^{13}C{^{15}N} REDOR NMR dephasing for samples prepared at intermediate pH values supports a model in which each register segregates into different fibrils, or, alternatively, populates larger domains within the same fibril. Although ^{13}C{^{15}N} REDOR NMR data cannot distinguish between these two possibilities, they clearly exclude a fully random mixing of the two registers.[24] The work of Meier and co-workers has also revealed that small changes at the molecular level, such as side-chain protonation of glutamic acids along the peptide sequence, can have a large effect on the final fibril structure.[24] A similar phenomenon (i.e., protonation of glutamic and aspartic acids) has also been discussed by Tycko and co-workers for Aβ_{11-25} fibrils prepared at acidic conditions (pH 2.4), which have a different registry compared to pH 7.4 Aβ_{11-25} fibrils.[8] Nielsen and co-workers have further developed a useful approach based on symmetry principles, solid-state NMR, and XRD in studies of poly-

DOI: 10.1021/acs.biochem.5b01095
Biochemistry 2016, 55, 2065−2068

morphism of amyloid fibrils: eight classes of steric zippers in β-sheet pleated amyloid fibrils formed from short peptides have been identified.[25]

It has been also found that different arrangements of β-sheets in amyloid fibrils may lead to different (both ^{13}C and ^{15}N) chemical shift patterns. The chemical shifts depend on whether the side-chain points into or away from the zipper, leading to large chemical shift differences for "odd/even" combinations relative to "even/even" or "odd/odd" combinations of side-chains on the interacting surfaces of laminas.[25] Supported by TEM and ^{15}N CP/MAS NMR data reported here (Figures S12–S16), we hypothesize that the peptides studied in this work are also affected by these general paradigms of polymorphism of amyloid fibrils, i.e., "off-registry" shifts in combination with interlamina surface interactions in amyloid fibrils. We further note that, as shown by *in situ* AFM, different polymorphs of amyloid fibrils, such as the Arctic mutation of $A\beta_{1-40}$(E22G), may simultaneously grow in the same sample conditions.[26]

Conclusions. In summary, assisted by the resolving power of FTICR-MS, the ratios of ^{17}O enrichment of two amyloid peptides, $A\beta_{16-22}$ and $A\beta_{11-25}$, were quantified using their isotopic fine structures. By comparing to the corresponding $^{15}N\{^{17}O\}$REAPDOR NMR experiments, only about one-third to one-half of the Aβ peptides in these samples were found involved in the formation of the specific >C═^{17}O···H–^{15}N hydrogen bonds with their neighbor peptide molecules. We hypothesize that the rest of the molecules adopt amyloid fibril structures undergoing ± n off-registry shifts in β-sheets, which suggests a high degree of polymorphism exhibited by Aβ species in forming hydrogen-bonded networks.

Tandem mass spectrometry methods determined the isotope labeling site. This research expands the application of isotopic fine structure mass spectrometry in NMR research and demonstrates the unique value of ultrahigh resolution and high mass accuracy capabilities of FTICR-MS for applications in the NMR community requiring isotopic labeling.

■ ASSOCIATED CONTENT

Supporting Information

The Supporting Information is available free of charge on the ACS Publications website at DOI: 10.1021/acs.biochem.5b01095.

Figures S1–S16 and Tables S1–S12 as noted in text (PDF)

■ AUTHOR INFORMATION

Corresponding Author

*Fax: (+44) 24-765-241-12. E-mail: p.oconnor@warwick.ac.uk.

Funding

This work was supported by the Chancelors International Scholarships of Warwick, EPSRC (EP/J000302/1), the Foundation in memory of J. C. and Seth M. Kempe, and the Alzheimer's Foundation of Sweden. The UK 850 MHz solid-state NMR Facility used herein was funded by EPSRC and BBSRC (EP/F017901/1), the University of Warwick including via part funding through Birmingham Science City Advanced Materials Projects 1 and 2 supported by Advantage West Midlands (AWM) and the European Regional Development Fund (ERDF). Experimental Data are available at the Warwick Research Archive Portal: http://wrap.warwick.ac.uk/77887/.

Notes

The authors declare no competing financial interest.

■ ACKNOWLEDGMENTS

Special thanks are due to Dr. Yulin Qi and Dr. David Kilgour for phasing the spectra and useful discussions.

■ REFERENCES

(1) Lansbury, P. T., Costa, P. R., Griffiths, J. M., Simon, E. J., Auger, M., Halverson, K. J., Kocisko, D. A., Hendsch, Z. S., Ashburn, T. T., Spencer, R. G. S., Tidor, B., and Griffin, R. G. (1995) *Nat. Struct. Biol. 2*, 990–998.

(2) Benzinger, T. L. S., Gregory, D. M., Burkoth, T. S., Miller-Auer, H., Lynn, D. G., Botto, R. E., and Meredith, S. C. (1998) *Proc. Natl. Acad. Sci. U. S. A. 95*, 13407–13412.

(3) Tycko, R., and Ishii, Y. (2003) *J. Am. Chem. Soc. 125*, 6606–6607.

(4) Petkova, A. T., Leapman, R. D., Guo, Z. H., Yau, W. M., Mattson, M. P., and Tycko, R. (2005) *Science 307*, 262–265.

(5) Tycko, R. (2011) *Annu. Rev. Phys. Chem. 62*, 279–299.

(6) Benzinger, T. L. S., Gregory, D. M., Burkoth, T. S., Miller-Auer, H., Lynn, D. G., Botto, R. E., and Meredith, S. C. (2000) *Biochemistry 39*, 3491–3499.

(7) Balbach, J. J., Ishii, Y., Antzutkin, O. N., Leapman, R. D., Rizzo, N. W., Dyda, F., Reed, J., and Tycko, R. (2000) *Biochemistry 39*, 13748–13759.

(8) Petkova, A. T., Buntkowsky, G., Dyda, F., Leapman, R. D., Yau, W. M., and Tycko, R. (2004) *J. Mol. Biol. 335*, 247–260.

(9) Antzutkin, O. N., Iuga, D., Filippov, A. V., Kelly, R. T., Becker-Baldus, J., Brown, S. P., and Dupree, R. (2012) *Angew. Chem., Int. Ed. 51*, 10289–10292.

(10) Hung, I., Uldry, A.-C., Becker-Baldus, J., Webber, A. L., Wong, A., Smith, M. E., Joyce, S. A., Yates, J. R., Pickard, C. J., Dupree, R., and Brown, S. P. (2009) *J. Am. Chem. Soc. 131*, 1820–1834.

(11) Shi, S. D.-H., Hendrickson, C. L., and Marshall, A. G. (1998) *Proc. Natl. Acad. Sci. U. S. A. 95*, 11532–11537.

(12) Nikolaev, E. N., Jertz, R., Grigoryev, A., and Baykut, G. (2012) *Anal. Chem. 84*, 2275–2283.

(13) Liu, Q., Easterling, M. L., and Agar, J. N. (2014) *Anal. Chem. 86*, 820–825.

(14) Nakabayashi, R., Sawada, Y., Yamada, Y., Suzuki, M., Hirai, M. Y., Sakurai, T., and Saito, K. (2013) *Anal. Chem. 85*, 1310–1315.

(15) Qi, Y., Witt, M., Jertz, R., Baykut, G., Barrow, M. P., Nikolaev, E. N., and O'Connor, P. B. (2012) *Rapid Commun. Mass Spectrom. 26*, 2021–2026.

(16) Drader, J. J., Shi, S. D. H., Blakney, G. T., Hendrickson, C. L., Laude, D. A., and Marshall, A. G. (1999) *Anal. Chem. 71*, 4758–4763.

(17) Qi, Y., Barrow, M. P., Li, H., Meier, J. E., Van Orden, S. L., Thompson, C. J., and O'Connor, P. B. (2012) *Anal. Chem. 84*, 2923–2929.

(18) Qi, Y., Thompson, C., Van Orden, S., and O'Connor, P. (2011) *J. Am. Soc. Mass Spectrom. 22*, 138–147.

(19) Naito, Y., and Inoue, M. (1996) *Int. J. Mass Spectrom. Ion Processes 157-158*, 85–96.

(20) Mitchell, D. W., and Smith, R. D. (1995) *Phys. Rev. E: Stat. Phys., Plasmas, Fluids, Relat. Interdiscip. Top. 52*, 4366–4386.

(21) Caravatti, P., and Allemann, M. (1991) *Org. Mass Spectrom. 26*, 514–518.

(22) Favrin, G., Irbäck, A., and Mohanty, S. (2004) *Biophys. J. 87*, 3657–3664.

(23) Xie, L., Luo, Y., and Wei, G. (2013) *J. Phys. Chem. B 117*, 10149–10160.

(24) Verel, R., Tomka, I. T., Bertozzi, C., Cadalbert, R., Kammerer, R. A., Steinmetz, M. O., and Meier, B. H. (2008) *Angew. Chem., Int. Ed. 47*, 5842–5845.

(25) Nielsen, J. T., Bjerring, M., Jeppesen, M. D., Pedersen, R. O., Pedersen, J. M., Hein, K. L., Vosegaard, T., Skrydstrup, T., Otzen, D. E., and Nielsen, N. Ch. (2009) *Angew. Chem., Int. Ed. 48*, 2118–2121.

(26) Norlin, N., Hellberg, M., Filippov, A., Sousa, A. A., Gröbner, G., Leapman, R. D., Almqvist, N., and Antzutkin, O. N. (2012) *J. Struct. Biol. 180*, 174–189.

DOI: 10.1021/acs.biochem.5b01095
Biochemistry 2016, 55, 2065–2068